JOURNAL OF CATALYSIS 127, 128–140 (1991)

On the Strength of Solid Acids

BENJAMIN UMANSKY, JOZSEF ENGELHARDT,[1] AND W. KEITH HALL[2]

Chevron Science Center, Department of Chemistry, University of Pittsburgh, Pittsburgh, Pennsylvania 15260

Received April 23, 1990; revised July 24, 1990

The objective of the present work was to establish the relative strengths of some common solid acids and to put them on a scale familiar to chemists. A modified spectrophotometric approach involving H_0 and H_R indicators was developed. The red-shifts of spectra from the adsorbed neutral forms of 4-nitrotoluene and 4-nitrofluorobenzene were used to deduce the equivalent H_2SO_4 concentrations. Thus, values of 70 to 80%, and 90 to 98% H_2SO_4 were determined for silica–alumina and HY preparations, respectively. HM preparations were found to be mild superacids (stronger than 100% H_2SO_4). On the other hand, H_2SO_4/ZrO_2 preparations had surface acidities about equivalent to 100% H_2SO_4, and SbF_5/silica–alumina was a superacid with $-14.5 < H_0 < -13.7$. These data were correlated with the catalytic activities of the solid acids expressed either as ln (reaction rate) at 370°C or as the temperature required to obtain 0.5% conversion of isobutane. The extent and nature of the secondary reactions also varied with the acidity. These results demonstrate that the *intensive* factor of the acidity (acid strength) dominated over the *extensive* factor (surface concentration of Brønsted sites) in controlling the acidity, and therefore the catalytic properties, of these solids.

INTRODUCTION

The manner in which Brønsted sites are introduced into zeolites via deamination of the NH_4^+ forms, and how such sites are transformed into Lewis sites by dehydroxylation accompanied by dealumination, has been understood for many years (*1, 2*) and has been confirmed by infrared studies of the spectra of adsorbed pyridine (*3*). Although these features were qualitatively known, as was the nature of the interaction of weaker bases such as olefins and aromatics with the Brønsted sites (*4*), it has only recently been recognized that paraffins may be directly protonated to initiate carbenium ion chains (*5–7*). McVicker *et al.* (*8*) were first to point out the virtues of isobutane as a reactant. The C_3 and C_4 carbenium ions which are formed from this substrate cannot undergo β-scission, thus greatly simplifying the product distributions which can be produced. They also reported that the products obtained over HY and other zeolitic materials differed distinctly from those obtained over amorphous silica–alumina catalysts and suggested that the former results were characteristic of superacid catalyts while the latter may have involved alkoxide intermediates. We have confirmed and extended their data to include the reactions of neopentane over a wide variety of zeolites (*6*), whereas Abbot and Wocjiechowski (*7*) have studied a wide variety of paraffin structures over an HY-zeolite. Presently it is fair to say that all of these experimental results are in fairly good agreement with one another although they have been interpreted somewhat differently by the authors.

A salient feature of the isobutane reaction is that the product compositions fall between two extremes (*6, 8*). The least active catalysts yield only the products of the pri-

[1] Permanent address: Central Institute for Chemistry of the Hungarian Academy of Sciences, Budapest, Hungary.

[2] To whom all correspondence should be addressed.

0021-9517/91 $3.00

mary decomposition reaction, H_2 and CH_4, together with the corresponding olefins C_4H_8 and C_3H_6. At the other extreme only paraffins are produced and in quantities which greatly exceed the hydrocarbon products formed in the primary (initiation) reaction as measured by $H_2 + CH_4$. This suggests that carbenium ion chains have been established since in this way much larger amounts of isobutane can be reacted by H^- transfer. The Y-zeolites tend to fall in between these extremes. A simple means of treating such data was devised (*9*). The reaction network has been described in more detail elsewhere (*10*). In the present work we have attempted to quantify the corresponding acid strengths with which to correlate the catalytic data.

Recently, it was shown (*11*) that spectroscopic determination of peak maxima is essential for the correct estimation of acid strength using adsorbed H_0 indicators. The visual observation of color can be very misleading. It was reported that the peak positions of the protonated forms of the indicators varied by no more than a few nanometers regardless of whether the species were formed in H_2SO_4 or on the surface of various adsorbents. The peak positions of spectra of the neutral forms of the indicators, however, were not constant; they shifted to longer wavelengths as the interaction between the indicator and the catalyst became stronger. It may be supposed that these observations resulted from a site selective chemisorption on the acidic centers of the adsorbent and that protonation occurred only when this interaction became sufficiently strong. Bathochromic spectral shifts of more basic H_0 indicators (up to a $pK_{BH+} = -8.2$) have been previously recorded by Leftin and Hobson (*12*) and by Drushel and Sommers (*13*). Kotsarenko *et al.* (*14*) observed similar shifts with less basic indicators (up to a $pK_{BH+} = -11.35$). In all of these cases the spectral shifts were associated with the increasing interaction energy between the indicator and the site. In the present work nomographs were established relating the peak positions obtained from the perturbed neutral forms of 4-nitrotoluene (4NT) and 4-nitrofluorobenzene (4NFB) to the concentrations of aqueous H_2SO_4 solutions which in turn can be related to their known H_0 values (*15–17*). Hammett and Deyrup (*18*) defined H_0 in a way analogous to pH; i.e., it is a measure of the acidity which is independent of the acid tested. Walling (*19*) took advantage of this principle to extend the use of the H_0 function to solid acids. Many others have followed suit. Thus, in the present work it has been convenient (and proper) to calibrate the acidities of our solid acids to those of sulfuric acid solutions having the same H_0 values. Further justification for this concept may be drawn from the results obtained.

EXPERIMENTAL

Catalysts. The catalysts studied, their origins, and their physicochemical properties are listed in Table I where they are grouped according to catalyst type. Mostly they were used as received following a standard pretreatment procedure. For the reader's convenience, the suppliers' designations are given in the second column, where the SiO_2/Al_2O_3 or the Si/Al ratios are given in parentheses and the specified percentage Na_2O are in brackets. Our own analytical data for these samples are given systematically in the remainder of the table and should be used in consideration of the experimental results. With one or two notable exceptions, the lattice aluminum concentrations (Al_F/g) were in fairly good agreement with the total aluminum concentration (Al_T/g) obtained by emission analysis. Moreover, their pore volumes generally indicated good crystallinity. Davison 62 silica gel, Houdry M-46, and Nikki-631-L silica–aluminas were used. The Houdry M-46 was from the same batch used in much of our earlier work. The starting material for H-Y(8.1) was a Linde LZ-Y62 sieve (NH_4NaH) which was twice exchanged with NH_4Cl to reduce the Na content. This material was dealuminated following a standard procedure of hydro-

TABLE 1[a]

Description of the Catalysis[b]

Catalyst	Chemical analysis (wt%)			$Al_T/g^c \times 10^{-20}$	$Al_F/g^c \times 10^{-20}$	Si/Al[c] (*F*/*W*)	Pore vol.[c] (surface area)	Source
	SiO_2	Al_2O_3	Na_2O					
Silica–aluminas								
1 M-46	87.5	12.5	n.d.	14.8	—	—	(270)	Houdry Co.
2 N-631-L	87.0	13.0	n.d.	15.4	—	—	(500)	NIKKI Co.
Y-Zeolites								
3 LZ-210(6) [2.0][d]	77.2	20.8	2.0	22.8	22.8	3.4	0.33	Linde Co.
4 LZ-210(6) [0.45]	78.4	21.1	0.45	23.2	22.8	3.4	0.33	Linde Co.
5 LZ-210(6) [<0.1]	78.8	21.2	0.02	23.3	22.8	3.4	0.33	Linde Co.
6 H-Y (8.1)	90.2	9.3	<0.3	10.9	10.8	13.2	0.30	LZ-Y62
7 LZ-210(9) [0.1]	84.0	15.9	0.1	16.8	17.6	4.7	0.33	Linde Co.
8 LZ-210(12) [0.46]	86.9	12.7	0.46	14.8	14.6	6.0	0.33	Linde Co.
9 LZ-210(12) [0.1]	87.3	12.7	0.1	14.9	14.6	6.0	0.33	Linde Co.
10 LZ-Y82	75.7	24.1	0.46	28.3	15.8	5.2	0.32	Linde Co.
ZSM-5 preparations								
11 JRC-Z5-7OH	97.9	2.1	<0.1	2.1	2.1	46.1	0.18	CSJ[e]
12 H-ZSM-5(35)	97.6	2.4	<0.01	2.8	2.8	34.7	0.18	Mobil Corp.
13 H-ZSM-5(40)	97.5	2.5	0.1	2.8	2.8	34.6	0.17	CRIC[f]
14 H-ZSM-5(25)	96.5	3.4	0.1	4.1	3.8	25.4	0.19	CRIC
15 JRC-Z5-25H	93.4	6.5	0.1	7.2	6.7	13.9	0.20	CSJ
16 H-ZSM-5(15)	94.0	6.0	<0.1	7.1	6.3	14.8	0.17	A.P.[g]
Mordenites								
17 JRC-Z-HM10	85.3	14.6	0.1	17.3	17.0	4.9	0.18	CSJ
18 JRC-Z-HM15	89.7	10.2	0.1	12.0	12.0	7.5	0.18	CSJ
19 JRC-Z-HM20	92.1	7.8	0.1	9.2	9.2	10.0	0.18	CSJ
20 LZ-M8	90.9	9.1	<0.1	10.6	10.6	8.9	0.18	Linde Co.
Others								
21 β-zeolite	95.0	4.3	0.31	5.04	—	—	0.31	PQ Corp.
22 ZrO_2/H_2SO_4	—	—	—	—	—	—	(85)	
23 M-46/SbF_5	87.5	12.5	—	—	—	—	(<270)	In house

[a] Results of more detailed catalytic tests may be found elsewhere (*9*, *10*).

[b] The physicochemical data below were obtained in house on the preparations actually studied. They should be used in making cross comparisons among catalysts.

[c] Al_T/g is the total Al per gram determined by chemical analysis: Al_F/g is the framework Al from ^{29}Si-MASNMR; Si/Al (*F*/*W*) is this ratio calculated from the NMR data, and Pore vol. (surface area) is given in cm^3/g or (m^2/g) and was calculated from BET measurements.

[d] These samples are labeled with the suppliers' designations. The SiO_2/Al_2O_3 (and sometimes the Si/Al ratios) are given in parentheses and the Na_2O percentages in brackets.

[e] Catalysis Society of Japan.

[f] Central Research Institute for Chemistry of the Hungarian Academy of Sciences.

[g] Air Products and Chemicals Company, Allentown, PA.

thermal treatment and then exchanged twice with NH_4NO_3. The extra-lattice alumina was then extracted with acid (1.0 *N* HCl at 60°C for 2 hr).

The LZ-Y210(12.0) [0.46], LZ-Y210(9) [0.1], and LZ-Y210(6) [2] were supplied by Linde. These materials were treated at 90°C with 1.0 *M* ammonium acetate to reduce

their sodium contents. After drying at 120°C these samples were calcined at 500°C for 5 hr. The suppliers' designations frequently indicated the SiO_2/Al_2O_3 ratio in the parentheses; in other cases these are Si/Al ratios. This is irrelevant, however, as the framework Si/Al ratios as determined by ^{29}Si MAS NMR are given in the eighth column.

The ZrO_2/H_2SO_4 was prepared from $Zr(OH)_4$ made by hydrolysis of zirconyl chloride (Aldrich >98%) with aqueous NH_4OH at pH 10. The precipitate was washed and then dried at 110°C overnight. The sulfate was introduced by pouring 15 ml of 1 *N* sulfuric acid per gram of $Zr(OH)_4$ onto the filter paper. This material was dried at 110° overnight and then loaded into the reactor where it was calcined for 3 h at 650°. The final catalyst contained 4.0% SO_4 and had a surface area of 85 $m^2\ g^{-1}$.

The SbF_5 promoted M-46 SiO_2–Al_2O_3 catalyst (M-46/SbF_5) was made as follows. The M-46 was calcined in a stream of dry O_2; the temperature was raised 5°C/min to 500°C, where it was maintained for 12 hr. Following this treatment the solid was evacuated to 10^{-6} Torr before cooling to room temperature. The SbF_5 was then vacuum transferred onto the pretreated catalyst by exposure to its sublimation pressure at room temperature for 10 min and evacuated at the same temperature. This procedure was repeated 3 times before the preparation was given a final evacuation at 50°C.

Spectroscopic measurements. The methods used have been reported in detail elsewhere (*11*). Thin self-supporting wafers (*7–10* mg/cm^2) were pressed from the powdered materials. These were introduced into quartz UV cells with attachments through graded seals to a conventional high-vacuum system, where pretreatment was carried out. The cooled pretreated samples were immersed without exposure to air in 4 cm^3 of degassed *n*-heptane to enhance their transparency. Measured amounts of indicator were then introduced, after the baseline spectra were recorded from the blank. The spectrum from the adsorbed indicator was obtained by subtraction of the blank from the final spectra and correction for any unadsorbed indicator using the computer attachment of the spectrometer (#8450A Hewlett–Packard diode ray spectrometer). The software of this instrument made possible the determination of the position of the peak maximum with an absolute accuracy of ±1 nm. In general, the amounts of indicator added amounted to less than 1% of the lattice aluminum present so that the system should not be perturbed by the adsorption. For the present purposes, only the positions of the peak maxima were required. The pK_{BH+} values of 4NT and 4NFB are −11.3 and −12.4, respectively. Their spectroscopic peak positions in the neutral form are at 264 and 255 nm and in their protonated forms at 377 and 367 nm. In a few cases the preparations were not sufficiently transparent to obtain reliable data. In these cases the peak maxima were obtained from diffuse reflectance spectra using a Beckman Acta MVI spectrometer fitted with the Praying Mantis DR attachment. The accuracy of these determinations of peak maxima was estimated as ±10 nm.

The concentrations of 4NT and 4NFB were adjusted to obtain about 2.8×10^{18} and 5.6×10^{18} molecules/g, respectively. Thus, for the zeolites investigated, the order of 10^{-3} molecules/Al_F was available for adsorption. It was not possible to make such determinations on the H-ZSM-5 preparations; on these, the indicators were not adsorbed from the *n*-heptane solutions at room temperature, presumably because of their small pore openings.

Reagents and gases. Linde "extra dry" grade O_2 and prepurified dried N_2 from Matheson were used. The O_2 was passed through a column containing calcined 5A molecular sieve and anhydrous $CaSO_4$. The N_2 was passed through an indicating oxytrap 4004H from All Tech, to remove any oxygen from the reactant gas.

For the catalytic studies, reactant gas was a mixture of 10% isobutane (instrument grade) in 90% prepurified dried N_2 (Matheson). Impurities related to isobutane were 0.2% of propane plus *n*-butane. No olefins were detectable by GLC with FID detector. The indicators were purchased from Aldrich Chemical Company and used for preparation of dilute solutions without further purification. The solvent used was *n*-heptane (Mallincroft spectroscopic grade).

Catalytic tests. Catalytic tests were carried out at atmospheric pressure in a continuous-flow quartz U-tube reactor using the entrance half of the tube as a preheater. The catalyst (400 mg) was packed between quartz wool plugs and pretreated as described elsewhere (*9*); it was given a final treatment in flowing dry O_2 at 500°C overnight before being flushed and cooled to the desired reaction temperature in a flow of dried high-purity N_2. At a preselected temperature, 10% isobutane in N_2 was fed at a fixed space velocity ($F/W = 1.12 \times 10^{-5}$ mole g^{-1} s^{-1}) except when it was necessary to adjust it to maintain a low, but measurable, total percentage conversion of isobutane (below ~5%). Under these conditions deactivation of the catalysts with time on stream was not detected.

The product was analyzed with on-line GLC for H_2 and C_1 to C_6 hydrocarbons. When a steady state was reached, another temperature was tested (in the steady state) without interrupting the feed. The temperature was changed randomly, up or down, and in this way Arrhenius plots were constructed for the isobutane conversion rates. Hence, the values used were all obtained below 5% total conversion and differential reaction rates were calculated as $C_i = X_i(F/W)$, where (F/W) was the space velocity of isobutane calculated as mole g^{-1} s^{-1}. The total conversion rate of isobutane was then calculated as $C = (\frac{1}{4})\Sigma_i jC_i$, excluding isobutane, where j is the number of carbon atoms in each of the ith product molecules; thus C is the differential rate of conversion of isobutane to all observed products. Although it is known (*8*) that the *primary* initiation reactions are first order in isobutane and the *secondary* hydride transfer reactions are second order, the zeroth order approximation has been used to calculate activation energies for the low conversion data.

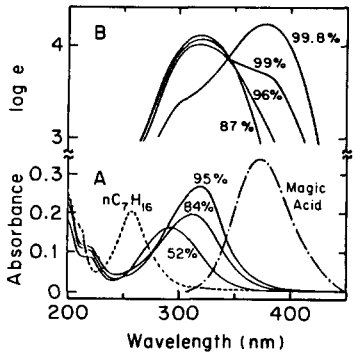

FIG. 1. (A) Spectra of 4-nitrotoluene in n-C_7H_{16}, in 52, 84, and 95% H_2SO_4, and in magic acid (SbF_5/HSO_3F = 1). (B) Spectra of 4-nitrotoluene in 86, 96, 99, and 99.8% H_2SO_4 (taken from Ref. (*17*); e is the extinction coefficient determined as described therein).

RESULTS

Spectra from 4-nitrotoluene (4NT) and 4-nitrofluorobenzene (4NFB) in 16, 30, 52, 70, 84, 90, and 95% H_2SO_4 and in n-C_7H_{14} or in magic acid (SbF_5/HSO_3F = 1) were recorded. The indicator concentrations were kept approximately constant at about 10^{-6} M and in each case the same aqueous acid (or *n*-heptane) was used in the reference cell in the double beam mode. Some of these spectra from 4NT solutions are shown in Fig. 1A. They show the shift in the peak maxima toward longer wavelength as the acid concentration is increased from 52 to 95%. Shown above (Fig. 1B) are data taken from Ref. (*17*). The peak maximum for 87% is in good agreement with our data; a second band appeared as a shoulder in 96% acid and this grew in 99% H_2SO_4; it became the principal peak in 99.8% acid. This peak at about 376 nm was from the protonated form of the indicator which was the only species observed in magic acid. These spectra delin-

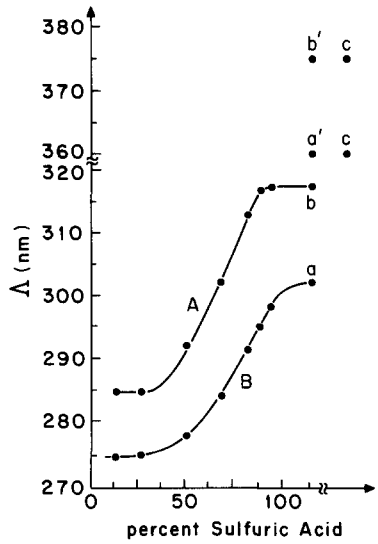

FIG. 2. Peak positions of 4-nitrotoluene (A) and 4-nitrofluorobenzene (B) in different concentrations of H_2SO_4; both peaks appeared in fuming H_2SO_4 (a,a' and b,b'). Only the protonated form, BH^+, appeared in magic acid (c).

eate the typical behavior of these systems. The protonated form of the indicator is in equilibrium with the unprotonated form (peak position 318 nm; not at 275 nm as in *n*-heptane).

Similar behavior was found for 4NFB in aqueous sulfuric acid solutions. The peak positions of both indicators shifted to longer wavelengths as the acid strength was increased. The peak maxima from these spectra are plotted as the nomographs in Fig. 2. These data can be converted into H_0 values using published data (*15*, *16*). For the present purposes we reference the peak positions obtained from the several catalysts to these nomographs and find the equivalent concentrations of H_2SO_4. From these data the corresponding H_0 values can be deduced. Although this procedure may seem arbitrary, it does provide an idea of the strength of the solid acid in terms familiar to chemists. The validity of this approach must be inferred from the results it produces. Note, however, that (a) this concept is implicit whenever H_0 values are used to describe catalyst acidity and (b) single values for this parameter are produced by this approach rather than ranges.

Data for a number of catalyst preparations as obtained from the two indicators are listed in Table 2. The equivalent sulfuric acid concentrations listed in columns 4 and 5 serve as a cross check on the method. The agreement is quite good and the data reflect the poisoning by sodium in experiments 3–5 and in 6–8. Previously this difference was not detected by the bracketing method (*11*) because of the rather large differences in the pK_{BH+} values of the adjacent indicators. Interestingly the HM catalysts qualify as mild superacids having $H_0 \approx -12.4$. Our measurements using DRS also showed that ZrO_2/H_2SO_4 is not a strong superacid catalyst as has been claimed (*20*); instead, it approximates 100% H_2SO_4 as might have been anticipated. Finally, not only does the nomograph method appear to provide a more precise measure of the acidity than the bracketed method, a single measurement with one indicator should be sufficient for determining the acidity of a solid acid, now that the calibration has been done. However, the method could not be applied to SbF_5/M-46 because it, like magic acid, protonated both indicators. Instead, the bracketed method (*11*) was applied to deduce $-14.5 < H_0 < -13.7$.

The catalytic activity data expressed as rates of cracking (10^{-9} mole g^{-1} sec^{-1}) as a function of temperature are plotted in the Arrhenius fashion in Fig. 3. These results clustered into three groups. The least active catalysts were the amorphous silica/aluminas (runs 1 and 2). The most active catalysts were the HM series (runs 17–20) and the remaining catalysts fell in between. Shown are data for the HY catalysts (runs 3–10) and for the β-zeolite (run 21). For the sake of clarity those for the H-ZSM-5 catalysts (runs 11–16) were not plotted in Fig. 3 because these plots were superimposed on those for the HY, but had lower slopes (see Table 3). From these plots, the temperatures required to reach 0.5% conversion (rates of

TABLE 2

H_0 Values of the Strongest Acid Sites of Catalysts Deduced from the Spectral Shift of Adsorbed 4-Nitrotoluene and 4-Nitrofluorobenzene, Having pK_{BH+} of -11.3 and -12.4, Respectively

No.	Catalyst	Peak position (nm)		$\%H_2SO_4/H_2O$		$-H_0$[a]
		4NT	4NFB	4NT	4NFB	
—	Silica gel	285	274	<30	<30	≤3
1	M-46	303	285	68	70	5.8
2	N-631-L	302	286	66	71	5.6
3	LZ-210(6) [2]	316	299	89	93	10.0
4	LZ-210(6) [0.45]	317	300	90	94	10.5
5	LZ-210(6) [0.1]	318	303	97	~100	12.0
6	H-Y (8.1)	318	299	97	93	10.0
7	LZ-210(9) [0.1]	318	301	>97	97	11.0
8	LZ-210(12) [0.46]	317	299	96	93	10.0
9	LZ-210(12) [0.1]	320	302	98	~100	12.0
10	LZ-Y82	330	302	98	~100	12.0
19[b]	JRC-Z-HM10	318 & 375[c]	300 & 360[c]	>100	>100	12.4
20	LZ-M8	318 & 375[c]	300 & 360[c]	>100	>100	12.4
21	β	317	299	94	93	10.0
22	ZrO_2/H_2SO_4[d]	~320	~300	~100	~100	~12.0
Magic acid (1 : 1)		375	360	protonated BH^+		12.4

[a] Average from the two indicators. These values were obtained from the equivalent H_2SO_4 concentrations using the data from Refs. (*11, 12*).

[b] Catalysts nos. 11 to 18 could not be determined; on these catalysts the pore openings were too small to allow the base molecules to enter. This is further explained in Ref. (*10*).

[c] Both peaks were present.

[d] Diffuse reflectance spectrum was obtained for this nontransparent material.

conversion equal 0.5% of the feed rate) and/or the conversion rates at 370°C could be determined. These data are listed in Table 3 together with the corresponding activation energies and turnover frequencies (TOF) based on the lattice aluminum values. In agreement with earlier work (*8–10, 21*), amorphous silica/alumina catalysts produced principally CH_4, H_2, C_3H_6, and *i*-C_4H_8, i.e., the products of the primary monomolecular initiation reaction. At the other extreme the mordenites produced principally paraffins; only trace amounts of olefins were observed. The remaining catalysts formed mixtures of olefins and paraffins in relative amounts which depended on both the temperature and the conversion level. For these, excluding CH_4, olefin to paraffin ratios near unity were rather typical. An enormous difference in catalytic activity and selectivity with increasing acidity is evident. The catalytic rates increased by about six orders of magnitude in going from silica–alumina preparations to the H-mordenites.

The relationship between the temperature required for 0.5% conversion and $-H_0$ is shown in Fig. 4. Ward and Hansford (*22*) published a similar correlation which related the poisoning effect of Na^+ on the acidity to the temperature required to maintain a given conversion of *o*-xylene to its isomers. As indicated, if the mordenite data (points 19 and 20) are excluded, the data could be fitted with a straight line. Closely similar results were obtained when ln *C* was plotted vs $-H_0$; i.e., there was an approximately linear correlation for all of the data except for the catalysts falling in the superacid range (up to an H_0 value $= -12$). Here

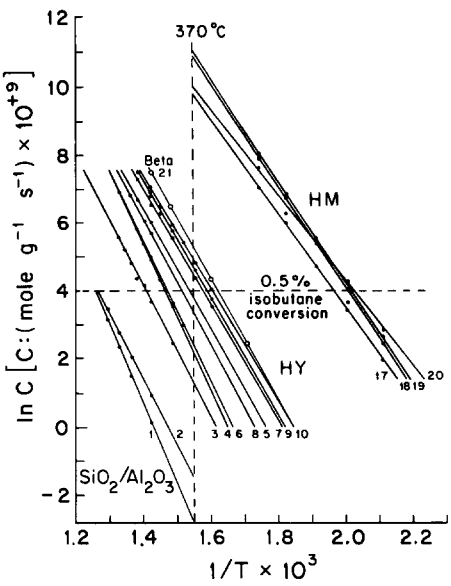

FIG. 3. Arrhenius plots for the total rate of i-C_4H_{10} conversion. Numbers refer to the catalysts listed in the tables.

again the mordenites were much too active to fit on this simple corelation, but see below.

Because the concentration of indicator in each of the sulfuric acid solutions was identical, the extinction coefficient could be observed to increase with the acidity in the range between 30 and 95% H_2SO_4. This is illustrated in Table 4. This behavior is reminiscent of effects in hydrogen bonding of bases to acids.

Figure 2 shows no spectral shift with these indicators in solutions containing less than about 30% sulfuric acid, whereas between 30 and 95% a nearly linear correlation exists between the position of the peak maxima and acid concentration. At still higher concentrations the indicators became protonated and new peaks appeared in the spectra corresponding to the protonated forms. In magic acid only the peak of the protonated indicator appeared.

DISCUSSION

In order to compare the acidity of zeolites with the acidity of inorganic oxyacids having the general formula of $(HO)_mXO_n$, Barthomeuf (*23*) noted that the acid strength increased with increasing n, but did not depend significantly upon m. Similar correlations were made for zeolites where the general formula was written as $(HO)_mTO_n$ with T being Al + Si, m = Al/(Al + Si), and $n = 2 - m$. The aluminosilicate structure restricts the number of oxygens per T atom to 2 and so limits n to this value. Therefore zeolites, with n values close to 2 (high Si/Al ratios), should be acids as strong as inorganic oxyacids with n values near 2, e.g., sulfuric acid [$(HO)_2SO_2$]. This was substantiated in the present work by the spectroscopic studies of the adsorbed indicator bases which showed that the acidity of such zeolites was in the range of concentrated to fuming H_2SO_4. As reported earlier (*6*), however, a more detailed examination of the data showed that the structure of zeolite has a very significant effect on its acidity. Among catalysts with identical, or almost identical, Si/Al ratios, e.g., [LZ-210(9)[0.1– vs JRC-Z-HM10 and LZ-210(12)[0.1] vs JRC-Z-HM15], the mordenites were found to be much stronger acids than the H-Y-zeolites, and this was reflected by the much higher catalytic activities reported herein.

The dashed lines of Figs. 5 and 6 are plots of the H_0 determinations for aqueous H_2SO_4 solutions taken from two different investigations (*15, 16*). To these the data of Gillespie (*24*) for fuming sulfuric acid solutions (hatched line) have been added. Note the sudden upward swing in the apparent acidity, $-H_0$, as 100% H_2SO_4 is approached. The abscissa above 100% is the mole percentage SO_3 with respect to H_2SO_4, i.e., the mole percentage of $H_2S_2O_7$. Thus, the discontinuity in $-H_0$ at about 100% H_2SO_4 occurs as H_2SO_4 molecules are being transformed into $H_2S_2O_7$ and the sudden increase in acidity corresponds, not to a higher concentration of protons per unit volume (as in dilute acids), but to an increase in anion size. Stated another way, the enhanced acidity results from a change in the *intensive* factor of the acidity, not in the *extensive* factor.

TABLE 3

Characteristic Values for Activity and Acidity of Different Catalysts

No.	Catalyst	Reaction temperature at 0.5% conversion (°C)	Rate of conversion at 370°C (mole · g^{-1} sec^{-1}) × 10^9	E_a kcal $mole^{-1}$	TOF at 370°C[a] × 10^6
1	M-46	522	0.06	48.2	
2	N-631-L	518	0.22	39.1	
3	LZ-210(6) [2.0]	437	3.7	39.7	1.2
4	LZ-210(6) [0.45]	410	9.0	42.9	2.5
5	LZ-210(6) [0.1]	378	13.4	35.4	3.5
6	H-Y (8.1)	406	11.0	42.0	6.2
7	LZ-210(9) [0.1]	362	90.0	34.0	32.1
8	LZ-210(12) [0.46]	387	30.0	37.5	13.1
9	LZ-210(12) [0.1]	356	110	33.4	45.2
10	LZ-Y82	349	148	32.6	57.0
11	JRC-Z5-70H	408	8.2	32.4	23.4
12	H-ZSM-5(35)	400	9.0	37.8	19.3
13	H-ZSM-5(40)	369	33.1	28.2	20.9
14	H-ZSM-5(25)	351	60.3	26.4	95.2
15	JRC-Z5-25H	319	181	24.6	162
16	H-ZSM-5(15)	311	221	25.0	211
17	JRC-Z-HM10	236	18000	27.8	6353
18	JRC-Z-HM15	225	59900	30.6	29950
19	JRC-Z-HM20	224	54200	32.3	35348
20	LZ-M8	221	22000	25.4	12453
21	β-Zeolite	346	180	42.1	—

[a] Calculated from the number of lattice aluminums corrected for those charges compensated by Na^+. This value was taken as the number of Brønsted sites.

Acidity is a generic term meant to imply the effectiveness of an acid for reaction with a given base. This property may be controlled by two different effects, the *extensive* and *intensive* factors, which are never completely separable. The former reflects the principle of mass action; it will always be present, but not necessarily dominant. The latter involves the strength of the individual acid sites in their interaction with various, particularly weak, bases. This factor will be evidenced by the interaction energy (or heat of adsorption) between the acid site and the base, by whether the base is protonated or not, and by the observable effects of this interaction on the spectra obtained from selectively chemisorbed bases. In some cases this may be the H-bonding shifts in the vibrational spectrum from the Brønsted sites effected by molecules such as C_2H_4 (*3*) or CO (*26*). In the present case changes in the intensive factor are reflected by the bathochromic shifts of the weakly basic indicators in the optical spectra (Fig. 2). Thus, below about 50% H_2SO_4 the "acid strength" is controlled by the extensive factor; be-

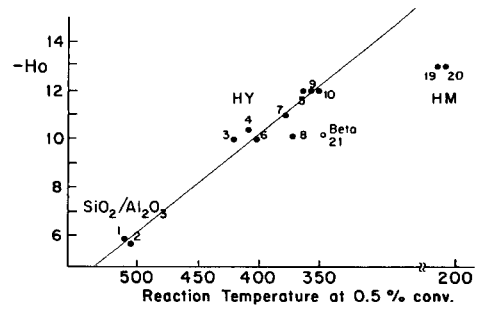

FIG. 4. Correlation of the temperature required for 0.5% conversion of i-C_4H_{10} with $-H_0$.

TABLE 4

Relative Absorbance of 4-Nitrotoluene in Solutions of Different Sulfuric Acid Concentration[a]

H_2SO_4 %	A_i/A_{16}
16	1.00
30	1.08
52	1.11
70	1.62
84	2.20
90	2.17
95	2.18

[a] A_i is the absorbance of 4NT in $i\%$ H_2SO_4 and A_{16} is the absorbance of 4NT in 16% H_2SO_4.

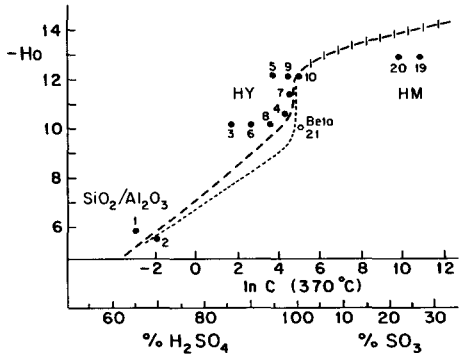

FIG. 6. Relationships between total rate of i-C_4H_{10} conversion at 370 C and percentage H_2SO_4 or fuming sulfuric acid and $-H_0$. Dashed lines from Refs. (*15*) and (*16*) and the hatched line from Ref. (*24*).

tween 50 and 90% the intensive factor becomes increasingly important and finally dominant as it becomes more and more difficult to increase the proton concentration (meq/cc) further. With 4NT and 4NFB the increasing intensive factor is reflected in the spectroscopic shifts up to the point where protonation of these bases starts to become detectable. With the zeolites, it is clearly the intensive factor which dominates. The SiO_2/Al_2O_3 ratio was varied from 6 to 9 to 12 with relatively small changes in the acidity and with the strongest of these acids having the lowest extensive factor (items 5, 7, and 9 of Table 2). Similarly, mordenites have acidity

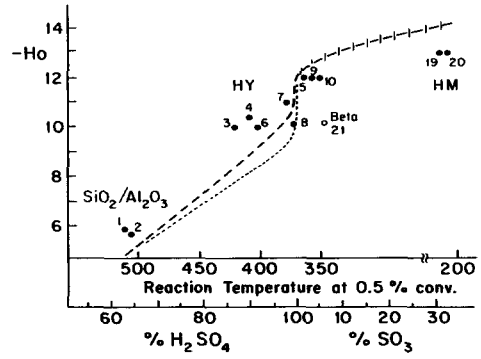

FIG. 5. Relationships between temperature required for 0.5% conversion of i-C_4H_{10} and percentage H_2SO_4 or fuming sulfuric acid and $-H_0$. Dashed lines taken from Paul and Long (*15*) and Jorgenson and Hartter (*16*) and the hatched line from Gillespie (*24*).

distinctly higher than that of Y-zeolites of similar Si/Al ratios and poisoning of a few percent of the Brønsted sites with Na^+ (*10, 24, 28*) or NH_3 (*9, 29*) has devastating effects on both the acidity and the catalytic activity.

The points plotted in Figs. 5 and 6 are the results of our experimental determinations with the abscissa scaled to fit the equivalent H_2SO_4 concentrations corresponding to the silica–alumina catalysts and the Y-zeolites. The H_0 values (ordinate) are the actual values determined for these catalysts. The activity data may be correlated to the acidity measurements better in this way than by a straight line or a monotonic curve. Interestingly this general behavior has been reported for other acid systems. A sudden large increase in acidity as measured by $-H_0$ was obtained as SbF_5 was added to HSO_3F (*25*). The apparent reason for this is the formation of larger anions represented as $SbF_5(FSO_3)^-$ which is paired with the Brønsted acid $H_2SO_3F^+$. For the present purposes the salient point is that the intensive factor of the existing Brønsted sites increases with the size of the charge compensating anion, possibly because the stabilization energy of the anion is increased by the larger anion volume.

When these concepts are translated to solid acids, such as the H-zeolites, certain deductions may be drawn. In general, and

as observed, the intensive factor should increase with the Si/Al ratio, although still larger effects may be obtained with changes in the structure of the solid. Moreover, within a given structure, a decrease in the extensive factor may overcompensate an increasing intensive factor in the limit of low Al concentration leading to the linear curves frequently observed (*23, 28–31*). Also, the formation of stable ions such as NH_4^+ by reaction of NH_3 with covalent Brønsted sites (*9, 29*) [or their replacement by Na^+ (*10, 27*)] would be expected to strongly reduce the intensive factor of the remaining sites by abruptly reducing the lattice anion volume.[3] These concepts are in general agreement with the experimental facts.

The red shifts of the unprotonated forms of the indicators are not understood in detail, but appear to be related to the strength of the interaction between the weak base and the strong acid. These are $\pi \rightarrow \pi^*$ transitions which are affected by this interaction. On silica gel, the spectral shift is minimal, if any occurs, but becomes appreciable with silica–alumina, and larger still with the HY preparations; the same large shifts occur with the HM catalysts, but accompanied by the band for the protonated form (Table 2). This behavior is reminiscent of the hydrogen bonding of the zeolite protons to such weak bases as C_2H_4, C_3H_6 (*3, 4*), C_6H_6 (*4, 32*), and CO (*30*). In all these cases large shifts of the OH stretching vibration to lower frequencies occurred and this was accompanied by an increased absorption coefficient and chemical reaction as the strength of the interaction (or temeprature) was increased. Interestingly, similar effects were observed in optical spectra from sulfuric acid solutions and on the solid acids as well. As the acidity was increased from 30% to 95–97% H_2SO_4, the strength of interaction between the weakly basic indicator and the proton of the acid became stronger and this was reflected by the shift of peak position of unprotonated 4NT from 285 to 318 nm. On further increase of the acidity, protonation of the indicator occurred and an equilibrium was established between the strongly polarized and the protonated forms. In magic acid, only the latter was present. As in the case of H-bonding, the proton is stretched from its rest position by interaction with the base, until the interaction becomes sufficiently strong for proton transfer (perhaps by tunneling) to occur. Now, both bands appear in the spectra. A deeper understanding of this phenomenon will require a good theoretical treatment.

In our previous paper (*11*) the weakest indicator base was sought which could be protonated by a given surface, and the next weaker one which could not. Using this "bracketed method" the acidity of catalysts could be ranked in the following sequence: for HM preparations, $-13.7 < H_0 < -12.4$; for HY and H-Beta, $-12.4 < H_0 - 8.7$, and for silica–alumina, $-8.7 < H_0 < -3.3$. Silica gel could not be bracketed so, $-3.3 < H_0$. The H_0 values determined from the peak position of 4NT and 4NFB (Table 2) invariably fell within these ranges. In addition, however, the new method discriminated between catalysts within these groups, e.g., betwen the same parent preparations having different Na^+ levels. Hence,

[3] A referee has asked for clarification on this point. It has long been recognized that electrons are delocalized over the charged lattice of a zeolite. The charge on the lattice is increased each time a covalent Brønsted sites is converted into a stable ion pair, e.g., NH_4^+/AlO_2^- or Na^+/AlO_2^-. Each additional electron put on the lattice in this way makes it energetically less favorable to add another, just as in charging an electrical condenser it costs more energy to add each subsequent electron than it did the one before it. The effect on catalytic activity will be dramatic because the *next* electron put on the lattice now corresponds to the formation of a metastable carbenium ion rather than a stable cation. The charge density on the lattice also increases with the framework Al concentration (decrease in the Si/Al) and it has been suggested that the catalytic activity is diminished as the Brønsted sites get closer together. We have suggested (*9, 29*) that the random replacement of Brønsted centers with charged ion pairs is another aspect of the same phenomenon; it results in an increase in the lattice charge per unit volume *or* a decrease in the volume available for electron delocalization (the anion volume).

the results obtained up to 95–97% of H_2SO_4 justify the use of the spectra shift method since: (a) the estimated values of H_0 obtained from 4NT and 4NFB are in quite good agreement with each other; (b) the H_0 values all fell within the ranges determined by the bracketed method; and (c) there is good correlation between these H_0 values and the activities of the several catalysts for isobutane cracking. For acidity higher than this, the new method did not yield such accurate acidity estimations, although it could be extended by the establishment of another nomograph with a still weaker base, e.g., 2,4-dinitrotoluene ($pK_{BH+} = -13.7$) or 2,4-dinitrofluorobenzene ($pK_{BH+} = -14.5$).

The indicator method as used in this work is presumably a measure of the intensive factor of the acidity. Only a few (the strongest) sites are detected and a 1 : 1 interaction between the Brønsted acid site and the weak indicator base is observed. Nevertheless, the H_0 values deduced from our experiments are frequently higher than those reported in the literature. As previously explained (*11*), this results from erroneous conclusions drawn from visual observations of color.

The H_0 scale of acidity was adopted for this work because it has been widely used in related literature. This concept is based upon a treatment developed from

$$B + H^+ \rightleftharpoons BH^+ \qquad (1),$$

and

$$K_{BH+} = a_{BH+}/a_B a_{H+}, \qquad (2),$$

where the a_i are the activities from which Hammett and Deyrup (*18*) defined

$$H_0 = pK_{BH+} - \log (BH^+)/(B). \qquad (3).$$

This formalism does not take explicit account of the role of the anion of the acid. The present work suggests that this is of critical importance in dealing with strong acids and that it would be more appropriate to develop a formalism based on

$$B + HA \overset{K_4}{\rightleftharpoons} BH^+ + A^-. \qquad (4).$$

It may easily be shown that

$$H_0 = pK_{BH+} - \log (HA)/(A^-) - \log K_4. \qquad (5).$$

Thus, the H_0 values measured for a single acid system directly reflect the relative values for a given anion. Note, however, when the anion changes so does K_4, giving a step change in H_0. It is suggested that this is responsible for the large (step) changes which occur near 100% H_2SO_4 and when SbF_5 is first added to HSO_3F. As the conjugate anion size increases (from HSO_4^- to $HS_2O_7^-$ or from SO_3F^- to $SO_3SbF_6^-$), K_4 undergoes a step increase, and this observed as a sharp decrease in H_0 as observed (Fig. 5 and 6). Better ways should be sought to take into account the concept of the *delocalization volume* of the electron left behind when a proton is donated to the base. Until this is done it is probably more reliable to draw comparisons with systems of variable acidity such as equivalent concentrations of H_2SO_4 or of SbF_5 in HSO_3F than to use the H_0 function.

ACKNOWLEDGMENTS

The authors are grateful to the U.S. Department of Energy, Division of Chemical Sciences, Office of Basic Energy Research for support of this work under Grant DE-FG02-87ER13774A000.

REFERENCES

1. Uytterhoeven, J. B., Christner, L. G., and Hall, W. K., *J. Phys. Chem.* **69,** 2117 (1965).
2. Kühl, G. H., *ACS Symp. Ser.* **40,** 96 (1977).
3. Liengme, B. V., and Hall, W. K., *Trans. Faraday Soc.* **62,** 521 (1966).
4. Cant, N. W., and Hall, W. K., *J. Catal.* **25,** 161 (1972); Kiselev *et al.*, *Trans. Faraday Soc.* **60,** 435 (1964); Basila, M. R., and Kantner, T. R., *J. Phys. Chem.* **71,** 467 (1967).
5. Haag, W. O., and Dessau, R. M., *in* "Proc. VIIIth Int. Congr. Catal. (Berlin)," p. 305, Vol. II, 1984.
6. Lombardo, E. A., Pierantozzi, R., and Hall, W. K., *J. Catal.* **110,** 171 (1988); **112,** 565 (1988); Lombardo, E. A., Gaffney, T. R., and Hall, W. K., *in* "Proc. 9th Inter. Congr. Catal., 1988" (M. J. Phillips and M. Ternan, Eds.). CIC Publications, Vol. 1, p. 412ff, 1988.
7. Abbot, J., and Wojciechowski, B. W., *J. Catal.* **113,** 353 (1988); 521 (1989); **115,** 1 (1989); **109,** 274 (1988); **104,** 80 (1987).
8. McVicker, G. B., Kramer, G. M., and Ziemiak, J. J., *J. Catal.* **83,** 286 (1983); **92,** 355 (1985).

9. Hall, W. K., Engelhardt, J., and Sill, G. A., *in* "Zeolites: Facts, Figures, Future" (P. A. Jacobs and R. A. van Santen, Eds.), p. 1253ff. Elsevier, Amsterdam, 1989.
10. Engelhardt, J., and Hall, W. K., *J. Catal.* **125,** 472 (1990).
11. Umansky, B. S., and Hall, W. K., *J. Catal.* **124,** 97 (1990).
12. Leftin, H. P., and Hobson, M. C., Jr., *Adv. Catal.* **14,** 115 (1963).
13. Drushel, H. V., and Sommers, A. L., *Anal. Chem.* **38,** 12/1723 (1966).
14. Kotsarenko, N. S., Karakchiev, L. G., and Dzis'ko, V. A., *Kinet. Katal.* **9,** 158 (1966).
15. Paul, M. S., and Long, F. A., *Chem. Rev.* **57,** 1 (1957).
16. Jorgenson, M. J., and Hartter, D. R., *J. Amer. Chem. Soc.* **85,** 878 (1963).
17. Brand, J. C. D., *J. Chem. Soc.,* 997 (1950).
18. Hammett, L. P., and Deyrup, A. J., *J. Amer. Chem. Soc.* **54,** 2721 (1932).
19. Walling, C., *J. Amer. Chem. Soc.* **72,** 1164 (1950).
20. Yamaguchi, T., and Tanabe, K., *Mater. Chem. Phys.* **16,** 67 (1986); Tanabe, K., *in* "Proc. 9th Int. Congr. Catal. (Calgary)," Vol. 1, p. 27, 1988; Arata, K., and Hino, M., Vol. 4, p. 1727, 1988; *J. Amer. Chem. Soc.* **101,** 6439 (1979); *React. Kinet. Catal. Lett.* **25,** 143 (1984); *Appl. Catal.* **18,** 401 (1985).
21. Lombardo, E. A., and Hall, W. K., *J. Catal.* **112,** 565 (1988).
22. Ward, J. W., and Hansford, R. C., *J. Catal.* **13,** 364 (1969).
23. Barthomeuf, D., *J. Amer. Chem. Soc.* **83,** 2 (1979); *J. Phys. Chem.* **83,** 249 (1979); *Mater. Chem. Phys.* **17,** 49 (1987).
24. Gillespie, R. J., Peel, T. E., and Robinson, E. A., *J. Amer. Chem. Soc.* **93,** 5083 (1972).
25. Olah, G. A., Surya Prakash, G. K., and Sommer, J., *in* "Superacids," p. 42f. Wiley, New York, 1985.
26. Knözinger, H., *in* "Proc. Inter. Symp., Acid-Base Catalysts, Sapporo, 1988"; Zaki, M. I., and Knözinger, H., *Mater. Chem. Phys.* **17,** 201 (1987).
27. Fritz, P. O., and Lunsford, J.H., *J. Catal.* **118,** 85 (1989); Sohn, J. R., Decanio, S. J., and Lunsford, J. H., *J. Phys. Chem.* **90,** 4847 (1986).
28. Beyerlein, R. A., McVicker, G. B., Yacullo, L. N., and Ziemiak, J. J., *J. Phys. Chem.* **92,** 1967 (1988).
29. Lombardo, E. A., Sill, G. A., and Hall, W. K., *J. Catal.* **119,** 426 (1989).
30. Bremar, H., Wendlandt, K. P., Chuong, U., Lohse, H., Stoch, H., and Beeker, K., *in* "Proc. 5th Int. Symp. Het. Catal. (Varma), 1983," Part I, p. 4356ff, 1983.
31. Haag, W. O., Lago, R. M.,and Weisz, P. B., *Nature (London)* **309,** 589 (1984); Olson, D. H., Haag, W. O., and Lago, R. M., *J. Catal.* **61,** 390 (1980).
32. Rouxhet, P. G., and Semples, R. E., *J. Chem. Soc. Faraday I* **70,** 202 (1974).